HHS Public Access

Author manuscript

Acta Biomater. Author manuscript; available in PMC 2023 June 20.

Published in final edited form as:

Acta Biomater. 2022 September 01; 149: 347–358. doi:10.1016/j.actbio.2022.06.042.

Intra-articular Injection of Flavopiridol-loaded Microparticles for Treatment of Post-Traumatic Osteoarthritis

Rapeepat Sangsuwan[a,d], **Jasper H.N. Yik**[b], **Matthew Owen**[c], **Gang-Yu Liu**[c], **Dominik R. Haudenschild**[b], **Jamal S. Lewis**[a,*]

[a]Department of Biomedical Engineering, University of California, Davis, CA 95616, USA

[b]Department of Orthopaedic Surgery, School of Medicine, University of California, Davis, CA 95616, USA

[c]Department of Chemistry, University of California, Davis, CA 95616, USA

[d]Laboratory of Natural Products, Chulabhorn Research Institute, Bangkok 10210, Thailand.

Abstract

Rapid joint clearance of small molecule drugs is the major limitation of current clinical approaches to osteoarthritis and its subtypes, including post-traumatic osteoarthritis (PTOA). Particulate systems such as nano/microtechnology could provide a potential avenue for improved joint retention of small molecule drugs. One drug of interest for PTOA treatment is flavopiridol, which inhibits cyclin-dependent kinase 9 (CDK9). Herein, polylactide-co-glycolide microparticles encapsulating flavopiridol were formulated, characterized, and evaluated as a strategy to mitigate PTOA-associated inflammation through the inhibition of CDK9. Characterization of the microparticles, including the drug loading, hydrodynamic diameter, stability, and release profile was performed. The mean hydrodynamic diameter of flavopiridol particles was ~15 μm, indicating good syringeability and low potential for phagocytosis. The microparticles showed no cytotoxicity *in-vitro,* and drug activity was maintained after encapsulation, even after prolonged exposure to high temperatures (60 °C). Flavopiridol-loaded microparticles or blank (unloaded) microparticles were administered by intraarticular injection in a rat knee injury model of PTOA. We observed significant joint retention of flavopiridol microparticles compared to the soluble flavopiridol, confirming the sustained release behavior of the particles. Matrix metalloprotease (MMP) activity, an indicator of joint inflammation, was significantly reduced by flavopiridol microparticles 3 days post-injury. Histopathological analysis showed that flavopiridol microparticles reduced PTOA severity 28 days post-injury. Taken altogether, this work demonstrates a promising, biomaterial platform for sustained small molecule drug delivery to the joint space as a therapeutic measure for post-traumatic osteoarthritis.

Graphical Abstract

*Corresponding author: Dr. Jamal S. Lewis, Associate Professor, Department of Biomedical Engineering, 1 Shields Avenue, Davis, CA 95616, USA, jamlewis@ucdavis.edu.

Declaration of Competing Interest

D.R.H and J.H.N.Y report a relationship with Tesio Pharmaceuticals, Inc. that includes stock ownership and board membership. D.R.H, J.H.N.Y, and J.S.L report patents (issued and pending) assigned to Regents of the University of California and Licensed by Tesio Pharmaceuticals. There is an institutionally approved plan for managing any potential conflicts arising from these relationships.

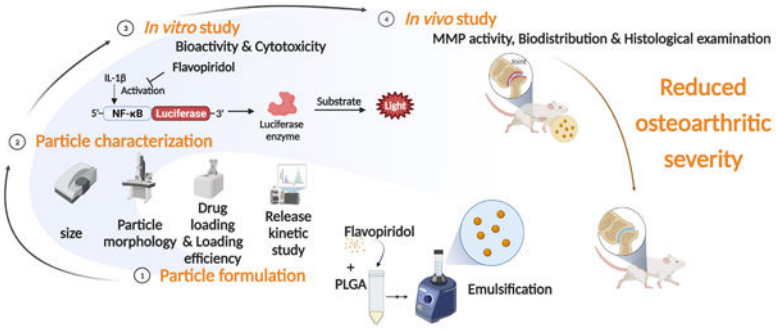

Keywords

Post-traumatic osteoarthritis (PTOA); PLGA; microparticles; inflammation; intra-articular; flavopiridol

1. Introduction

Post-traumatic osteoarthritis (PTOA) is a subtype of OA that begins with the deterioration of subchondral bone and cartilage after acute injuries such as anterior cruciate ligament (ACL) rupture, meniscus tear, and shoulder dislocation.[1–3] Approximately 12% of all symptomatic osteoarthritis (OA) in the United States will develop PTOA, which equates to approximately 5.6 million cases and up to $3 billion in annual treatment cost.[1, 2] Generally, PTOA initiates in a younger and more active population.[4, 5] Additionally, the incidence of ACL injuries is at least 10 times or higher among U.S. military members, compared to the reported rate for the U.S. population, and these patients have markedly increased risk of developing PTOA within 2–5 years.[6–8] Current clinical treatment of common knee injury focuses largely on relieving joint pain and stiffness. These palliative measures do not prevent the onset of cartilage and bone degeneration during the acute post-injury phase.[3, 9, 10] As such, patients are typically afflicted with chronic pain, loss of function and mobility, and the associated financial burdens.[3, 9, 10] Emerging evidence suggests that if disease intervention occurs at an early stage, the long-term prognosis of disease is much improved.[3, 9, 10] In this vein, scientists have strived to identify and understand key cellular and molecular changes after joint injury, which could guide the development of effective treatments for PTOA.

Post-traumatic osteoarthritis is initiated at the molecular and cellular level immediately after joint damage. During the early injury response phase, a number of primary response genes and pro-inflammatory cytokines, such as interleukin (IL)-1β, IL-6, and tumor necrosis factor (TNF)-α, are rapidly induced on a time-scale of minutes to hours.[2, 11–13] These inflammatory mediators then increase the production of matrix degrading enzymes such as matrix metalloproteases (MMPs), collagenases, aggrecanases, and cathepsins that cause secondary damage to various joint tissues during the late injury response phase.[14–17] The enzymatic degradation of matrix initiates OA via a cascade of destructive events: 1) reducing the stiffness and elasticity of cartilage, 2) increasing hydraulic permeability of cartilage, 3) increasing the accessibility of remaining cartilage matrix structures to enzymatic digestion,

4) thickening of the subchondral bone plate, 5) prompting structural changes to the underlying trabecular bone, 6) inducing formation of osteophytes and heterotopic bone, and 7) synovial tissue hypertrophy and initiating fibrosis. Attenuating these early injury responses could prevent irreversible molecular damage to the joint tissues and decrease the likelihood of PTOA development.[14–16]

The cyclin-dependent kinase 9 (CDK9) has been studied recently as a target for inhibition of inflammation. It is a serine/threonine kinase that forms the catalytic core of the positive transcription elongation factor b, which is necessary for RNA polymerase II (pol II)-dependent transcription of mRNAs.[18] This kinase is critical for stimulating transcription elongation of core inflammatory signal genes and its activity is the rate-limiting step for transcriptional elongation of primary response genes.[17] Previously, we showed that flavopiridol, a well-characterized pharmacological CDK9 inhibitor, inhibited inducible nitric oxide synthase (iNOS) and a broad range of inflammatory mediator gene expressions under pro-inflammatory stimuli.[19] Moreover, the activation of catabolic genes MMP-1, 3, 9, 13, and, ADAMTS(a disintegrin and metalloproteinase with thrombospondin motifs)-4, and −5 were dampened by flavopiridol.[20] These results demonstrated that flavopiridol can be used as an effective agent to prevent the activation of acute inflammatory response and catabolic pathways in cartilage and strongly suggested that this small molecule could provide a route for pharmacological intervention.

With respect to pharmacological intervention, localized intra-articular (IA) therapies are now seen as a much-preferred route than systemic therapy for OA. Intra-articular treatment has distinct advantages over systemic delivery, including lower overall doses, fewer systemic and adverse effects, as well as direct delivery of an active drug to the joint space that renders higher bioavailability.[21–23] However, intra-articularly injected drugs are rapidly cleared from the synovial fluid via the associated lymphatics and vasculature. The half-life of drugs administered via this route ranges from 1 to 13 hours, depending on the size of drugs.[24] Because of the short residence time in the intra-articular space, patients often receive multiple drug administrations, which introduces additional risks of adverse effects or joint damage.

Alternatively, microsphere biomaterial-based technologies have emerged as new platforms for offering sustained drug release and circumventing drug resistance. Of the various polymers used to make these drug delivery vehicles, poly lactic-co-glycolic acid (PLGA) is perhaps the most popular on account of its biodegradability, biocompatibility, high encapsulation capacity, as well as the ability to entrap hydrophilic and lipophilic drugs.[25] Moreover, PLGA has been approved by both the U.S. Food and Drug Administration (FDA) and European Medicine Agency (EMA) for the use in human, making the regulatory hurdle for derived vehicles significantly less challenging.[26]

Herein, we hypothesized that intra-articular delivery of flavopiridol-encapsulating PLGA microspheres would reduce OA severity and could prevent PTOA by early attenuation of inflammation. We tested this hypothesis in a rat model of PTOA using our previously established tibial compression-induced knee injury method.[16, 21, 27]

2. Materials and methods

2.1 Microparticle fabrication, characterization, and stability

2.1.1 Fabrication of flavopiridol-loaded PLGA microparticles (FPs).—

The flavopiridol microparticles (FPs) were provided by Tesio Pharmaceuticals (Davis, CA), or prepared in Lewis lab using a single emulsion-solvent evaporation technique similar to the previously described protocol[28, 29]. Briefly, 100 mg of PLGA (Lactel B6013–2, Evonik, Essen Germany) was dissolved in 0.5 mL of methylene chloride. Flavopiridol and fluorescent dyes at 2.4% (g/g drugs/ polymer) were added into the polymer solution, and then added to 1 mL of 10% poly(vinyl alcohol) solution in water. The solutions were vortexed at a full speed of a vortex mixer for 30 s to form particles. The particle suspensions were transferred to 30 mL of 1% poly(vinyl alcohol) and the particles were pelleted, subsequently washed with water, lyophilized and stored at −20 °C for further use. For the microparticle preparation using a NanoAssemblr system (Precision NanoSystems, Vancouver, Canada), a syringe of ethyl acetate solution containing flavopiridol or fluorescent dye at 2.4% weight percent (g drug/g polymer) and 1 mg/mL PLGA, and another syringe of aqueous solution containing 0.1% poly(vinyl alcohol) were attached to the instrument. The solutions were dispensed into the microfluidic cartridge at the total flow rate of 4 mL/min. The particles were collected and washed as mentioned earlier. The blank particles (BPs) were also synthesized as a control in which no drug was added during the formulation. Size distribution was measured by an Accusizer model 770 optical particle sizer (Entegris, Billerica MA).

2.1.2 Loading efficiency and stability of Flavopiridol-loaded microparticles—

The loading efficiency was determined by first dissolving PLGA microparticles in DMSO, followed by measuring the drug absorbance or fluorescence intensity in this solution. The calculation of loading efficiency was performed using a standard curve of the absorbance (280 nm) of flavopiridol and the fluorescence intensity (excitation at 630 nm, emission at 680 nm) of Cy5-flavopiridol. The stability of flavopiridol in the microparticles was tested by subjecting the microparticles to varying temperatures (4, 25 and 60 °C) for 1–3 months. Flavopiridol bioactivity was tested using an assay based on inhibition of IL-1β-induced NF-κB luciferase activity.

2.1.3 Scanning Electron Microscopy Imaging.—

The particle geometry and size were determined using scanning electron microscopy (SEM) imaging using a field emission SEM (S-4100T, Hitachi High Technologies America, Inc., Pleasanton, CA). The sample preparation involved depositing 10 μL of PLGA particle dispersion in Milli-Q water onto an Al-stub, then washing with milli-Q water and drying. The dried sample was then coated with 10 nm of gold via sputter coating (Ted Pella Inc., Redding, CA) and transported to the SEM vacuum chamber. For SEM imaging, typical acceleration voltage and emission current were 2 kV at 10 μA, respectively, and images were processed in Image J. For time dependent SEM studies, we placed 4 mg of particles in 0.5 mL of 1X PBS buffer containing 0.2% (V/V) Tween-20 in a 1.5 mL Eppendorf tube at 37 °*C* with mixing at 80 rpm, and at selected time points of release we centrifuged the mixture (1500 rpm/5 min) to a pellet. The pellet was washed with 1 mL of water and 50 μL of fresh water was added to the pellet, and 10

μL of the particle suspension was drop cast on the sample. 500 μL of fresh release medium was added to the particle suspension and placed back under release conditions to be used in subsequent time points.

2.1.4 Synthesis of Cy5-labelled flavopiridol—Cy5-carboxylic acid (29 mg, 72.17 μmol), 1-Ethyl-3-(3-dimethylaminopropyl)carbodiimide, hydrochloride (EDC, 36.89 mg, 192.45 μmol) and 4-Dimethylaminopyridine (2.94 mg, 24.06 μmol) were added to a solution of flavopiridol (25 mg, 48.11 μmol) in anhydrous dimethylformamide. The reaction mixture was stirred under dry condition for 18 h, then the solvent was removed *in vacuo*. The reaction was purified by reversed phase HPLC using hexane/ethyl acetate and the fractions were dried under vacuum to afford 25 mg of a blue solid (60% yield). Using high-resolution mass spectrometry (ESI/Orbitrap), the molecular mass of the product was found to be 866.3990 m/z, which is close to the calculated mass of Cy5-labelled flavopiridol, ($C_{53}H_{57}ClN_3O_6^+$ ($[M]^+$), 866.3931 m/z) (Figure S3).

2.1.5 Synthesis of Cy7-labelled PLGA—The synthesis was modified from the previously reported protocol[30] Briefly, EDC (61 mg, 2.76 mmol) and *N*-hydroxysuccinimide (NHS, 31 mg, 1.4 mmol) were added to a solution of PLGA (500 mg, 23 μmol) in anhydrous dichloromethane. The reaction mixture was stirred under dry conditions for 1 h, then the polymer was precipitated with diethyl ether to remove residual NHS and EDC. The precipitated polymer was collected by centrifugation at 4,000 g for 5 min. The precipitation and centrifugation were repeated twice. The polymer pellet was then dried under vacuo for 30–60 min. The dried polymer was subsequently dissolved in anhydrous dichloromethane followed by the addition of Cy7-amine (16 mg, 727 μmol) and *N,N*-diisopropylethylamine (DIPEA, 47.5 mg, 2.16 mmol). The reaction was stirred for 18 h at room temperature and the precipitation/centrifugation were performed three times. The Cy7-labelled PLGA was collected, dried under vacuum, and stored at −20 °C for further use.

2.2 Human chondrocyte isolation and viability

To determine the effects of the microparticles on chondrocyte viability, primary human chondrocytes were isolated from discarded de-identified cartilage tissues obtained from end stage osteoarthritis patients undergoing elective total knee arthroplasty, (15 consented donors, age 44–80 years) and cultured in DMEM with 10% FBS as previously described. [31] Chondrocytes were seeded into 96-well plates at 7,000 cells per well and cultured with blank microparticles (BPs) or flavopiridol microparticles at various concentrations (0.5 – 4 mg/mL). The supernatant was collected over 6 days, and cell viability was assessed by quantifying lactate dehydrogenase release (LDH assay kit Thermo Fisher) following the manufacture's protocol.

2.3 NF-κB luciferase assay for flavopiridol bioactivity

To assess the bioactivity of flavopiridol, we quantified its inhibition of IL-1β-induced activation of an NF-κB luciferase reporter expressed in HEK293 recombinant cell line (BPS Bioscience). Cells were seeded into wells of either standard 96-well tissue culture plate (Corning) or transwell-96 plates at a density of 30,000 cells/well. Cells were allowed to attach for 24 h, then pretreated with flavopiridol or blank microparticles at various

concentrations of 0.25, 0.5, and 1 mg/mL for 24 h. For transwell experiments, the particles were added into the inserts. In some wells, free (not PLGA-encapsulated) flavopiridol was added to a final concentration of 300 nM. Cells were then treated with 10 ng/mL of IL-1β for 24 h, and analyzed for NF-κB luciferase activity using neolite reporter gene assay system (PerkinElmer) following the manufacture's instruction. The luciferase intensity was measured using a luminescence plate reader (Molecular Devices). Cell viability was assayed as described in section 2.2 using an LDH assay kit.

2.4 Release kinetics of flavopiridol in PBS and human synovial fluid

The release profiles of the flavopiridol from the PLGA microparticles was tested both in PBS and in synovial fluid. First, 4 mg of lyophilized flavopiridol microparticles were dispersed in 0.5 mL of PBS/0.2% Tween-20 aqueous solution at 37 °C. The Tween-20 solution was added to ensure sink conditions such that the dissolution medium can dissolve at least two times the amount of flavopiridol encapsulated. At selected time points, the suspension was centrifuged at 4000 rpm for 5 min and the supernatant was extracted for determination of flavopiridol concentration using UV-Vis spectroscopy (see section 2.1.2). The particles were then dispersed again in 0.5 mL fresh medium until the next time point. The *in vitro* release at a given time point, t, was quantified by the cumulative percentage of flavopiridol, defined as the total released divided by the total encapsulated flavopiridol, m_f. At each time point, the flavopiridol mass in the supernatant solution, m_t, was determined using UV-Vis measurements of its flavopiridol concentration. The cumulative percentage of flavopiridol was calculated using eq (1) by adding the amount of flavopiridol released at each time point until the designated time, t, then divided by the amount of flavopiridol encapsulated (m_f)

$$\text{Cumulative Release } (\%) = \frac{1}{m_f}\sum_{t=0}^{t=t_f} m_t \qquad \text{eq (1)}$$

Flavopiridol release kinetics in human osteoarthritis synovial fluid, was determined using slight modifications of a previous published protocol[32]. Human Osteoarthritis synovial fluid was purchased from Discovery Life Sciences (Santa Barbara, CA). Microparticles (2 mg) were added in 0.5 mL of synovial fluid. Standard flavopiridol were prepared in DMSO at a concentration of 7.5 mM and were diluted in microcentrifuge tubes containing synovial fluid (0.5 mL) at various concentrations (0.1–1 μM) and the samples including the standard were incubated at 37 °C for 1, 3, 7, 14, 28, and 32 d. After designated incubation time, the sample and standards were added to acetonitrile (1 mL) to extract flavopiridol and precipitate proteins. The samples were then vortexed for 30 s and centrifuged at 12,000 g, 4 °C for 10 min. The supernatant was collected and dried under vacuo. Samples were then reconstituted in 50% acetonitrile in water and analyzed by liquid chromatography–mass spectrometry (LC-MS) using a protocol previous reported[32]. The cumulative release was quantified using the peak intensity of flavopiridol detected in the synovial fluid by LC-MS and the calculation was done similarly based on eq (1).

2.5 Biodistribution of PLGA microparticles upon intra-articular administration

All animals were maintained and used in accordance with NIH guidelines and approved by UC Davis Institutional Animal Care and Use Committee (approval number 21870). Rats were housed two per cage, 20–26 °C ambient temperature, 12-hour light/dark cycle, with ad libitum access to food and water. Animals were monitored by husbandry staff at least once every day, with monthly healthcare checks by a veterinarian. A total of 14 Lewis rats (male, 12-week-old, Charles River) were used for biodistribution studies. The experiment consisted of 3 groups: 1) untreated control; 2) soluble Cy5-labeled flavopiridol treated group and; 3) Cy7-labelled PLGA particles with encapsulated Cy5-labeled flavopiridol treated group. The rats were intra-articularly injected with 0.7 mg of the Cy7-labelled PLGA particles with encapsulated Cy5-labeled flavopiridol. As a control, a cohort of Lewis rats were injected with an equal dose of soluble Cy5-labeled flavopiridol. After the injection, mice were imaged using a whole-body imager (IVIS-200) at various time points (30 min, 4 h, 24 h, 48 h and 72 h). After 3 days, rats were euthanized, and the liver and kidneys dissected and assessed for the presence of fluorescence using an IVIS Spectrum Imaging System (PerkinElmer) under isoflurane anesthesia and monitoring the fluorescent signal of Cy5 and Cy7 using excitation/emission wavelengths of 640/700 nm and 745/800 nm, respectively. Circular regions of interest (ROI) encasing the knee joints were created, and the average radiant efficiency [p/s/cm^2/sr]/[μW/cm^2] in the ROI was calculated as a measure of fluorescent signal intensity using Living Image software 4.2 (PerkinElmer).

2.6 Non-invasive mechanical injury rat model of osteoarthritis

A total of 49 Lewis rats (male, 12-week-old, Charles River) were used for this experiment. The experiment consisted of 3 groups: 1) uninjured control; 2) injured and vehicle treated; and 3) injured and drug treated. Osteoarthritis was induced in the right knee by a tibial compression to rupture the anterior cruciate ligament (ACL) as described in a mouse model,[16] except with scaled up holding platens to fit a rat knee. Briefly, animals were anesthetized using isoflurane, and the right knee was placed at a flexed angle between the holding platens positioned within an electromagnetic material testing machine (Bose ElectroForce 2100, Eden Prairie, MN), and subjected to a dynamic axial compressive load (1 mm/s loading rate) to a target compressive load of 85N. This loading method causes a transient anterior subluxation of the tibia relative to the distal femur. The ACL tear was verified by an audible “snap”, and a corresponding abrupt change in the force displacement curve profile on the Bose ElectroForce instrument. Immediately after injury, 50 μL of flavopiridol-loaded or blank microparticles (0.8 mg particles) were administered by intra-articular injection.

2.7 In-vivo imaging of MMP activity

A total of 20 Lewis rats were used for detection of MMP activity. Intra-articular levels of MMP activity were assessed as an indication of inflammatory and catabolic processes. At day 1 post-injury, while under isoflurane anesthesia, both knees of each animal received an intra-articular injection 50 μL of MMPSense 750FAST (PerkinElmer, Boston, MA) resuspended in PBS as recommended by the manufacturer. Animals were then placed in an IVIS Spectrum Imaging System (PerkinElmer) under isoflurane anesthesia, and the

fluorescent signal of MMPSense750 monitored using excitation/emission wavelengths of 745/800nm. Circular regions of interest (ROI) encasing the knee joints were created, as described in the biodistribution study.

2.8 Histological analysis

At 3 days and 4 weeks post-injury, animals were euthanized by carbon dioxide asphyxiation. Both knees were dissected, fixed in 4% paraformaldehyde for 48 h, and stored in 70% ethanol. Samples were demineralized in 10% formic acid for 4 weeks, thoroughly rinsed in water, and paraffin-embedded. Sagittal sections of (4 μm) of the medial tibiofemoral joint were stained with hematoxylin and eosin and graded for synovitis on a scale of 0–9[33]. In addition, 4 weeks samples were stained with Safranin-O and Fast-Green and scored for OA using the modified Mankin scoring system[34], which consists of a combined score of 0–23 based on the following four categories: cartilage surface integrity (0–10); cellularity (0–4); cell cloning (0–4); and safranin O staining (0–5).

2.9 Statistical Methods

Statistical analyses were performed for multiple comparison using a one-way ANOVA. Statistical significance was determined by a one-way analysis of variance (ANOVA), followed by Tukey' s multiple-comparison test. For two group comparison, the data distribution was first tested for normality using the Shapiro–Wilk test. If the data were normally distributed, the means of each treatment group were compared using the Student's t-test (unpaired). Conversely, for the data distribution that was not normal, Mann-Whitney U test (unpaired) was used to compare the difference between two groups. Differences were considered significant if $p \leq 0.05$ using the Prism software (Version 8, GraphPad). Error bars represented mean ± standard error of the mean (S.E.), unless otherwise indicated.

3 Results

3.1 Fabrication and characterization of flavopiridol-loaded microparticles

Flavopiridol-loaded PLGA microparticles were formulated using a single emulsion technique in-house, and injection-grade material was provided by Tesio Pharmaceuticals. The properties of the microparticles including size, morphology, drug loading, and stability were investigated, and were comparable between the two sources. Microparticle size affects polymer degradation and, therefore rate of drug clearance from the synovial capsule. The hydrodynamic radius of MPs was constrained to approximately 10–20 μm, which is considered to be injectable and unphagocytosable.[35–37] The results showed the mean hydrodynamic diameter of the microspheres (generated by Tesio Pharmaceuticals) was ~ 14.9 μm, as determined by an Accusizer (Table 1). The morphology and shape of the microparticles was confirmed to be smooth and spherical, respectively, through SEM analysis (Figure 1). Flavopiridol was successfully loaded into the particles up to 1.2% of mass concentration and the loading efficiency was 50%, calculated from the actual mass of compound added (Table 1). Additionally, particles were also synthesized in Lewis laboratory. Several variables including time of emulsification and amount of surfactant were identified, and the optimized condition as described above. With this optimized protocol, particles with characteristics that parallel those produced by Tesio Pharmaceuticals

were formulated. The preparation methods between a vortex mixer and a Nanoassemblr system for MP preparation were also compared (Table 1). The result showed that vortexing gave better yields and loading efficiencies than those made by the Nanoassemblr system. Therefore, the vortex method was chosen for the remainder of experiments. For the biodistribution study, the fluorescently-labelled microparticles were fabricated using Cy5-labelled flavopiridol. Increased Cy5-labelled flavopiridol in the starting solution improved the loading efficiency and loading amount. The fluorescently-labeled microparticles with loaded flavopiridol comparable to the non-labeled microparticles were selected for use in the biodistribution study.

3.2 Viability of human chondrocytes exposed to flavopiridol-loaded microparticles

The effect of flavopiridol-loaded microparticles on the cytotoxicity in human chondrocytes was assessed using an LDH assay. The blank (unloaded) microparticles (BPs), as well as the drug-loaded particles showed no toxicity to the cells at the tested concentrations (Figure 2B).

3.3 Biological property and stability of flavopiridol microparticles

Various storage temperatures and times (4, 25 and 60 °C for 1–3 months) were evaluated for long-term stability of microparticles loaded with flavopiridol (Figure 2A). Two types of plates, a transwell plate or a regular plate, were used in this study to illustrate that the source of bioactivity was the compound released from the particles, and not from direct contact between the cells and the FPs. Unsurprisingly, there was no significant difference between the two experimental settings. The viability of the cells after 24 hours with the FPs was first assessed to confirm that the effects on NF-κB activity did not result from toxicity (Figure S1). As expected, IL-1β treatment increased NF-κB activity, and the IL-1β-induced increase was inhibited by soluble flavopiridol and by flavopiridol microparticles, but not blank microparticles. This indicates that flavopiridol released from the microparticles retained its biological activity after encapsulation (Figure 2C–D). Flavopiridol microparticles retained their biological activity even after extended storage at higher temperatures (Figure 2E). It must be noted that FPs stored at 60 °C showed a color change to yellow and the particle dispersion in media was different to the control. The color of the solution of microparticles kept at 60 °C was clear yellow, whereas the color of FPs stored at other conditions remained white and cloudy in texture (Figure S2).

3.4 Release kinetics of flavopiridol microparticles in PBS and human synovial fluid

The *in vitro* release profile of flavopiridol from the microparticles was characterized in PBS and human synovial fluid. Microspheres loaded with flavopiridol demonstrated typical linear release characteristics for PLGA with approximately 80–90% of the flavopiridol released by day 30 regardless of the immersion fluid (Figures 3B). SEM images showed that the microparticle morphology changed over time, in a manner consistent with their degradation and flavopiridol release during incubation in PBS at 37 °C (Figures 3C).

3.5 Biodistribution of flavopiridol MPs

The biodistribution of flavopiridol microparticles was assessed in rat knee (stifle) joints using dual fluorescently-labelled flavopiridol and fluorescently labeled microparticles. We

first synthesized Cy5-flavopiridol and Cy7-PLGA using EDC chemistry (Figure 4A). The encapsulation of Cy5-flavopiridol with Cy7-PLGA was then performed and the characterization is reported in Table 1. As expected, soluble Cy5-flavopiridol fluorescent intensity rapidly declined, whereas microparticle-encapsulated Cy5-flavopiridol and Cy7-PLGA microparticles retained most of their fluorescence intensity in the joint out to at least 3 days (Figure 4B–E). There were significant differences in the drug retention between soluble Cy5-flavopiridol and Cy5-flavopiridol in FPs at 24, 48 and 72 h. Some organs, including liver and kidneys, were harvested and assessed for drug- and PLGA-associated fluorescence. Results showed that significant drug accumulation occurred in the liver for the soluble Cy5-flavopiridol treatment, whereas fluorescence levels were below detection limits for the livers and kidneys of rats given PLGA encapsulated Cy5-flavopiridol (Figure 4F).

3.6 Evaluation of Flavopiridol microparticles in a rat ACL injury model of PTOA

Matrix metalloproteinases are proteolytic enzymes that catalyze the degradation of various proteins in the extracellular matrix, and therefore can indicate the level of inflammation and enzymatic degradation within a tissue[39]. MMPsense was used to quantify the presence of MMPs and activity in joints. After ACL rupture on the right knee, rats were injected with the described MP treatments and/or MMPsense (Figure 5A). In the rat PTOA model, the non-surgical joint injury caused a substantial increase in the MMPsense fluorescence intensity in the injured right knee relative to the uninjured left knee of the same animal, indicating that injury increased the local MMP activity (Figure 5B). At the early post-injury time points, intra-articular injection of flavopiridol microparticles markedly reduced the *in vivo* MMP activity (Figures 5C–E).

3.7 Histopathology following treatment with flavopiridol microparticles

Given the promising signs of reduced inflammation due to application of FPs, we next assessed the potential of flavopiridol microparticles to limit osteoarthritis progression in a rat knee injury model (Figure 6). In vehicle-treated animals, knee injury markedly increased the synovitis score ($p<0.0001$). In contrast, treatment with flavopiridol microparticles significantly reduced the synovitis score at 3 days and 28 days post-injury ($p<0.05$). Next, osteoarthritis was evaluated histologically based on the Modified Mankin's score on a scale of 0–23. Results showed that knee injury markedly increased the severity of osteoarthritis in vehicle-treated animals. Treatment with flavopiridol microparticles reduced osteoarthritic scores significantly at the femoral condyle, and a similar trend of reduced OA severity was observed in the tibia although the tibial scores did not reach statistical significance.

4 Discussion

We have developed a controlled-release microparticle formulation encapsulating a CDK9 inhibitor (flavopiridol). Flavopiridol microparticles were successfully formulated using a single emulsion-solvent evaporation technique. Particulate size is often a crucial factor for accumulation, retention and penetration of particles in the knee joint space. Nanoparticles with a hydrodynamic <250 nm are flushed from synovial capsules freely. Particulates ranging from 100 nm to 5 μm are phagocytosed by macrophages and other phagocytes[35–37, 41–43]. As such, we engineered our Flavopiridol-loaded microparticles to have a

hydrodynamic diameter of about 15 μm, which is also suitable for syringe delivery into the intra-articular space[35–37, 41–43].

Safety is the key element in drug development; therefore, the cytotoxicity of flavopiridol microparticles was amongst the first primary outcomes to be assessed. Flavopiridol and blank microparticles show no toxic effects following extended cultures with human chondrocyte cells. This is not surprising, as many previous studies have shown that PLGA particulate formulations are not harmful to a variety of cells[44–46]. Further, we confirmed that the bioactivity of the flavopiridol remained after the encapsulation, using cell-based assay based on inhibition of IL-1β-induced NF-κB luciferase activity. The fabrication process of PLGA particles is known to be quite harsh and can often denature the encapsulated drug, rendering it useless for its intended purpose. However, that is not the case here and encapsulation did not interfere with the bioactivity of flavopiridol. The long-term stability and bioactivity of the flavopiridol microparticles was also investigated. Even after 90 days at 60 °C, FPs still release active flavopiridol comparable to that stored at −20 °C, suggesting this formulation easily negates the necessity of the cold chain system. A weakness of this assay is that we did not measure the release kinetics in the samples stored at higher temperatures. Another critical metric for the ultimate application of this formulation is the drug release profile of flavopiridol microparticles, which we evaluated in both phosphate-buffered saline and human osteoarthritic synovial fluid. The data demonstrates that, irrespective of fluid, the sustained release profile occurred over the course of 30 days, which is comparable or even longer than similar constructs[47, 48]. This is explained by that the difference in particle constitution and size. The prolonged release of flavopiridol from our microparticles suggests that a single intra-articular injection may suffice for maintenance of effective drug concentration within the joint capsule to achieve the outcome of reduced inflammatory gene expression.

Moreover, we observed a linear release profile of flavopiridol from PLGA microparticles, again regardless of the immersion fluid, which is consistent with release of small, oil-soluble drugs from PLGA particles formulated in previous studies[26, 29].

Central to our hypothesis is that flavopiridol microparticles remain largely within the knee joint space to allow for sustained delivery of flavopiridol to this inflamed area. Through independently fluorescently-labelling flavopiridol and PLGA, we were able to visualize the location of these agents in real time *in vivo* after the injection, and determine the clearance rate of both the small molecule drug and PLGA biomaterial. The slower rate of clearance of Cy5-flavopiridol entrapped in microparticles compared to the soluble compound could be due to the protection of the encapsulated flavopiridol by microparticles and the steady and slow release of the compound. PLGA showed the slowest rate of clearance as it has the most abundance among the others sample and also a chemical degradation process takes longer time than the release of entrapped small molecule. We also collected liver and kidneys and imaged them to trace the compound or degraded polymers in these organs. Flavopiridol accumulation in the liver was only evident for the soluble Cy5-flavopiridol treatment, indicating rapid clearance from the knee joint following administration. The higher concentration of the free unencapsulated flavopiridol in the liver at early times may

cause adverse effects[49], highlighting another benefit of the microparticle formulation as a safer drug delivery strategy.

We evaluated the therapeutic efficacy of the flavopiridol microparticles in preventing PTOA in a rat model that employs a noninvasive technique to introduce ACL rupture. Since MMP is the major proteases involved in cartilage degradation, MMP activity was used to visualize the inflammation stage after the acute injury[39]. A significant increase in MMP activity was observed in the injured group of rats compared to those uninjured, confirming that the enzymatic degradation in the joint occurred at the early stage of PTOA (2–3 days). Flavopiridol microparticles reduced the protease activity of MMPs 2–3 days post injury. Histological data suggests that both short- and long-term treatment are significantly effective as the flavopiridol microparticle-treated group had lower scores in both synovitis and Modified Mankin's scores. Taken together, these results indicated that intra-articular flavopiridol microparticle treatment is biologically active and efficacious in reducing synovitis and osteoarthritis severity. Finally, it has to the noted that the injury model used in this study is considered to be a relatively severe model of PTOA and with respect to knee damage, goes beyond what is typically observed in human patients with PTOA [27]. In addition, a limitation of this study is that we cannot rule out additional damage to other surrounding tissues/ ligament/tendon beside the ACL, leading to co-morbidities with confounding results in the long-term. With this context, the significant reduction in MMP activity and improved histopathological outcomes at acute time points is a hugely promising - the onset inflammation could be reduced using FPs. Future pharmacokinetic study including flavopiridol release after injection is required for optimization of drug treatment plan, in order to achieve the full potential of the drug treatment.

5 Conclusions

In summary, flavopiridol was successfully encapsulated in biocompatible PLGA microspheres of a hydrodynamic diameter that allows for delivery via syringe whilst circumventing phagocytosis. Following encapsulation, the biological activity of the flavopiridol was still intact and the particle formulation showed high stability, even at high temperatures, after storage for 1 – 3 months. Microspheres encapsulating flavopiridol slowly degraded, released the active flavopiridol into the joint capsule, and showed an improved joint residence time over the un-encapsulated flavopiridol in rat knee joints. More importantly, with the controlled-release properties, the microparticle construct showed no or low flavopiridol accumulation in liver and kidneys, unlike the unencapsulated free flavopiridol. In addition, the flavopiridol microparticles reduced the severity of PTOA at the early and later stages after joint injury. Altogether, the data in this study provides strong evidence for further development of this strategy as a promising disease-modifying anti-PTOA treatment.

Supplementary Material

Refer to Web version on PubMed Central for supplementary material.

Acknowledgments

This work was supported by the DOD (CDMRP Award PR171305) to D.H. and NIH (R01AI139399) to J.S.L.

6 References

[1]. Thomas AC, Hubbard-Turner T, Wikstrom EA, Palmieri-Smith RM, Epidemiology of posttraumatic osteoarthritis, Journal of athletic training 52(6) (2017) 491–496. [PubMed: 27145096]

[2]. Delco ML, Kennedy JG, Bonassar LJ, Fortier LA, Post-traumatic osteoarthritis of the ankle: a distinct clinical entity requiring new research approaches, Journal of Orthopaedic Research 35(3) (2017) 440–453. [PubMed: 27764893]

[3]. Anderson DD, Chubinskaya S, Guilak F, Martin JA, Oegema TR, Olson SA, Buckwalter JA, Post-traumatic osteoarthritis: improved understanding and opportunities for early intervention, Journal of orthopaedic research 29(6) (2011) 802–809. [PubMed: 21520254]

[4]. Valderrabano V, Hintermann B, Horisberger M, Fung TS, Ligamentous posttraumatic ankle osteoarthritis, The American journal of sports medicine 34(4) (2006) 612–620. [PubMed: 16303875]

[5]. Carbone A, Rodeo S, Review of current understanding of post-traumatic osteoarthritis resulting from sports injuries, Journal of orthopaedic research 35(3) (2017) 397–405. [PubMed: 27306867]

[6]. Weiss ND, Knee Ligaments: Structure, Function, Injury, and Repair, The Yale journal of biology and medicine 64(2) (1991) 194.

[7]. Buhl-Nielsen A, The epidemiology of anterior cruciate ligament injuries in athletes, Acta Orthop Scand 62(Suppl 243) (1991) 13.

[8]. Grimm PD, Mauntel TC, Potter BK, Combat and noncombat musculoskeletal injuries in the US military, Sports medicine and arthroscopy review 27(3) (2019) 84–91. [PubMed: 31361716]

[9]. Lotz MK, New developments in osteoarthritis: posttraumatic osteoarthritis: pathogenesis and pharmacological treatment options, Arthritis research & therapy 12(3) (2010) 1–9.

[10]. Riordan EA, Little C, Hunter D, Pathogenesis of post-traumatic OA with a view to intervention, Best Practice & Research Clinical Rheumatology 28(1) (2014) 17–30. [PubMed: 24792943]

[11]. Miller RE, Miller RJ, Malfait A-M, Osteoarthritis joint pain: the cytokine connection, Cytokine 70(2) (2014) 185–193. [PubMed: 25066335]

[12]. Kapoor M, Martel-Pelletier J, Lajeunesse D, Pelletier J-P, Fahmi H, Role of proinflammatory cytokines in the pathophysiology of osteoarthritis, Nature Reviews Rheumatology 7(1) (2011) 33–42. [PubMed: 21119608]

[13]. Murphy K, Weaver C, Janeway's immunobiology, Garland science 2016.

[14]. Rose BJ, Kooyman DL, A tale of two joints: the role of matrix metalloproteases in cartilage biology, Disease Markers 2016 (2016).

[15]. Lee JH, Fitzgerald JB, DiMicco MA, Grodzinsky AJ, Mechanical injury of cartilage explants causes specific time-dependent changes in chondrocyte gene expression, Arthritis & Rheumatism: Official Journal of the American College of Rheumatology 52(8) (2005) 2386–2395.

[16]. Christiansen BA, Anderson M, Lee CA, Williams J, Yik J, Haudenschild DR, Musculoskeletal changes following non-invasive knee injury using a novel mouse model of post-traumatic osteoarthritis, Osteoarthritis and cartilage 20(7) (2012) 773–782. [PubMed: 22531459]

[17]. Fowler T, Sen R, Roy AL, Regulation of primary response genes, Molecular cell 44(3) (2011) 348–360. [PubMed: 22055182]

[18]. Zhou Q, Yik JH, The Yin and Yang of P-TEFb regulation: implications for human immunodeficiency virus gene expression and global control of cell growth and differentiation, Microbiology and Molecular Biology Reviews 70(3) (2006) 646–659. [PubMed: 16959964]

[19]. Yik JH, Hu Z, Kumari R, Christiansen BA, Haudenschild DR, Cyclin-dependent kinase 9 inhibition protects cartilage from the catabolic effects of proinflammatory cytokines, Arthritis Rheumatol 66(6) (2014) 1537–46. [PubMed: 24470357]

[20]. Hu Z, Yik J, Cissell D, Michelier P, Athanasiou K, Haudenschild DR, Inhibition of CDK9 prevents mechanical injury-induced inflammation, apoptosis and matrix degradation in cartilage explants, European cells & materials 30 (2016) 200. [PubMed: 26859911]

[21]. Lockwood KA, Chu BT, Anderson MJ, Haudenschild DR, Christiansen BA, Comparison of loading rate-dependent injury modes in a murine model of post-traumatic osteoarthritis, Journal of Orthopaedic Research 32(1) (2014) 79–88. [PubMed: 24019199]

[22]. Evans CH, Kraus VB, Setton LA, Progress in intra-articular therapy, Nature Reviews Rheumatology 10(1) (2014) 11–22. [PubMed: 24189839]

[23]. Emami A, Tepper J, Short B, Yaksh TL, Bendele AM, Ramani T, Cisternas AF, Chang JH, Mellon RD, Toxicology evaluation of drugs administered via uncommon routes: intranasal, intraocular, intrathecal/intraspinal, and intra-articular, International journal of toxicology 37(1) (2018) 4–27. [PubMed: 29264927]

[24]. Gerwin N, Hops C, Lucke A, Intraarticular drug delivery in osteoarthritis, Advanced drug delivery reviews 58(2) (2006) 226–242. [PubMed: 16574267]

[25]. Cohen S, Yoshioka T, Lucarelli M, Hwang LH, Langer R, Controlled delivery systems for proteins based on poly(lactic/glycolic acid) microspheres, Pharm Res 8(6) (1991) 713–20. [PubMed: 2062800]

[26]. Makadia HK, Siegel SJ, Poly lactic-co-glycolic acid (PLGA) as biodegradable controlled drug delivery carrier, Polymers 3(3) (2011) 1377–1397. [PubMed: 22577513]

[27]. Christiansen BA, Guilak F, Lockwood KA, Olson SA, Pitsillides AA, Sandell LJ, Silva MJ, van der Meulen MC, Haudenschild DR, Non-invasive mouse models of post-traumatic osteoarthritis, Osteoarthritis and cartilage 23(10) (2015) 1627–1638. [PubMed: 26003950]

[28]. Lewis JS, Dolgova NV, Zhang Y, Xia CQ, Wasserfall CH, Atkinson MA, Clare-Salzler MJ, Keselowsky BG, A combination dual-sized microparticle system modulates dendritic cells and prevents type 1 diabetes in prediabetic NOD mice, Clinical Immunology 160(1) (2015) 90–102. [PubMed: 25842187]

[29]. Allen R, Chizari S, Ma JA, Raychaudhuri S, Lewis JS, Combinatorial, Microparticle-Based Delivery of Immune Modulators Reprograms the Dendritic Cell Phenotype and Promotes Remission of Collagen-Induced Arthritis in Mice, ACS Applied Bio Materials 2(6) (2019) 2388–2404.

[30]. Gu F, Langer R, Farokhzad OC, Formulation/preparation of functionalized nanoparticles for in vivo targeted drug delivery, Micro and Nano Technologies in Bioanalysis, Springer 2009, pp. 589–598.

[31]. Haudenschild DR, Chen J, Pang N, Steklov N, Grogan SP, Lotz MK, D'Lima DD, Vimentin contributes to changes in chondrocyte stiffness in osteoarthritis, J Orthop Res 29(1) (2011) 20–5. [PubMed: 20602472]

[32]. Phelps MA, Rozewski DM, Johnston JS, Farley KL, Albanese KA, Byrd JC, Lin TS, Grever MR, Dalton JT, Development and validation of a sensitive liquid chromatography/mass spectrometry method for quantitation of flavopiridol in plasma enables accurate estimation of pharmacokinetic parameters with a clinically active dosing schedule, Journal of Chromatography B 868(1–2) (2008) 110–115.

[33]. Krenn V, Morawietz L, Häupl T, Neidel J, Petersen I, König A, Grading of chronic synovitis—a histopathological grading system for molecular and diagnostic pathology, Pathology-Research and Practice 198(5) (2002) 317–325. [PubMed: 12092767]

[34]. Moody HR, Heard BJ, Frank CB, Shrive NG, Oloyede AO, Investigating the potential value of individual parameters of histological grading systems in a sheep model of cartilage damage: the Modified Mankin method, Journal of anatomy 221(1) (2012) 47–54. [PubMed: 22591160]

[35]. Liang LS, Wong W, Burt HM, Pharmacokinetic study of methotrexate following intra-articular injection of methotrexate loaded poly (L-lactic acid) microspheres in rabbits, Journal of pharmaceutical sciences 94(6) (2005) 1204–1215. [PubMed: 15858840]

[36]. Greis P, Georgescu H, Fu F, Evans CH, Particle-induced synthesis of collagenase by synovial fibroblasts: An immunocytochemical study, Journal of orthopaedic research 12(2) (1994) 286–293. [PubMed: 8164103]

[37]. Simkin PA, Nilson KL, Trans-synovial exchange of large and small molecules, clinics in rheumatic diseases 7(1) (1981) 99–129.

[38]. Vey E, Rodger C, Meehan L, Booth J, Claybourn M, Miller AF, Saiani A, The impact of chemical composition on the degradation kinetics of poly (lactic-co-glycolic) acid copolymers cast films in phosphate buffer solution, Polymer degradation and stability 97(3) (2012) 358–365.

[39]. Mehana E-SE, Khafaga AF, El-Blehi SS, The role of matrix metalloproteinases in osteoarthritis pathogenesis: An updated review, Life sciences 234 (2019) 116786. [PubMed: 31445934]

[40]. Khella CM, Horvath JM, Asgarian R, Rolauffs B, Hart ML, Anti-inflammatory therapeutic approaches to prevent or delay post-traumatic osteoarthritis (PTOA) of the knee joint with a focus on sustained delivery approaches, International Journal of Molecular Sciences 22(15) (2021) 8005. [PubMed: 34360771]

[41]. Wigginton SM, Chu BC, Weisman MH, Howell SB, Methotrexate pharmacokinetics after intraarticular injection in patients with rheumatoid arthritis, Arthritis & Rheumatism: Official Journal of the American College of Rheumatology 23(1) (1980) 119–122.

[42]. Bonanomi M, Velvart M, Stimpel M, Roos K, Fehr K, Weder H, Studies of pharmacokinetics and therapeutic effects of glucocorticoids entrapped in liposomes after intraarticular application in healthy rabbits and in rabbits with antigen-induced arthritis, Rheumatology international 7(5) (1987) 203–212. [PubMed: 3423619]

[43]. Levick J, A method for estimating macromolecular reflection by human synovium, using measurements of intra-articular half lives, Annals of the rheumatic diseases 57(6) (1998) 339–344. [PubMed: 9771207]

[44]. Singh V, Singh S, Das S, Kumar A, Self WT, Seal S, A facile synthesis of PLGA encapsulated cerium oxide nanoparticles: release kinetics and biological activity, Nanoscale 4(8) (2012) 2597–2605. [PubMed: 22419352]

[45]. Bee S-L, Hamid ZA, Mariatti M, Yahaya B, Lim K, Bee S-T, Sin LT, Approaches to improve therapeutic efficacy of biodegradable PLA/PLGA microspheres: a review, Polymer Reviews 58(3) (2018) 495–536.

[46]. Qi F, Wu J, Li H, Ma G, Recent research and development of PLGA/PLA microspheres/nanoparticles: A review in scientific and industrial aspects, Frontiers of Chemical Science and Engineering 13(1) (2019) 14–27.

[47]. Elsaid KA, Ubhe A, Shaman Z, D'Souza G, Intra-articular interleukin-1 receptor antagonist (IL1-ra) microspheres for posttraumatic osteoarthritis: in vitro biological activity and in vivo disease modifying effect, Journal of experimental orthopaedics 3(1) (2016) 1–10. [PubMed: 26915001]

[48]. Zhang Z, Bi X, Li H, Huang G, Enhanced targeting efficiency of PLGA microspheres loaded with Lornoxicam for intra-articular administration, Drug delivery 18(7) (2011) 536–544. [PubMed: 21812757]

[49]. Kahn ME, Senderowicz A, Sausville EA, Barrett KE, Possible mechanisms of diarrheal side effects associated with the use of a novel chemotherapeutic agent, flavopiridol, Clinical Cancer Research 7(2) (2001) 343–349. [PubMed: 11234889]

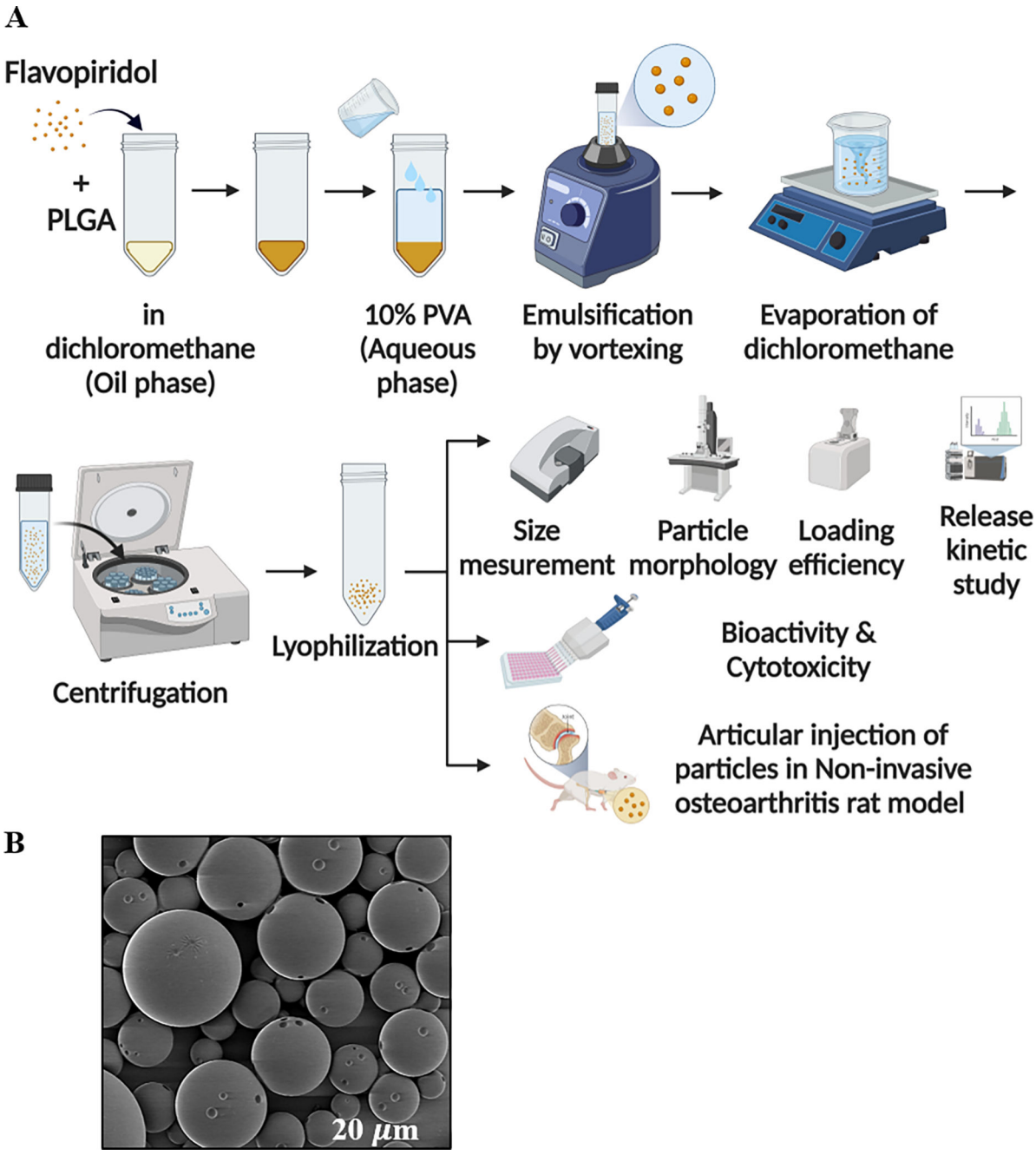

Figure 1. Preparation and characterization of flavopiridol-loaded PLGA particles.

A schematic depicting particle preparation, and characteristic properties of the generated particles are provided (A, Table 1) An SEM image of FPs (B). The scale bar (in white) represents 20 μm.

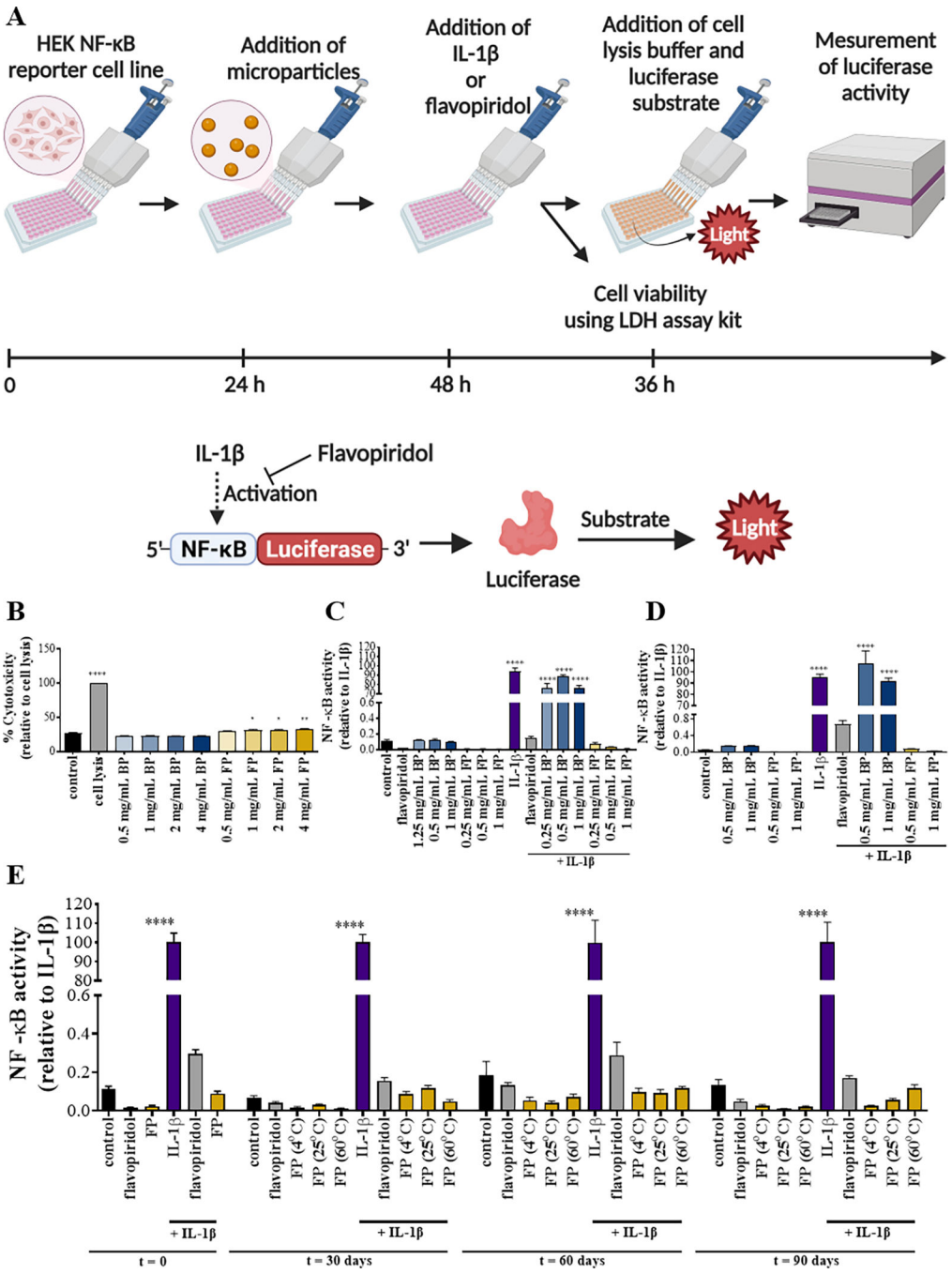

Figure 2. NF-κB activity of flavopiridol-loaded microparticles (FPs).

Methods used to determine the viability and bioactivity of FPs (A). Cytotoxicity of PLGA particles encapsulating flavopiridol was evaluated (B). NF-κB luciferase activity of PLGA particles encapsulated with flavopiridol in experiment settings performed in a regular plate (C) or in a transwell plate (D). Reporter cells were treated with media, soluble flavopiridol, IL-1β, blank MPs and/or flavopiridol-loaded MPs and the supernatants were collected and analyzed for NF-κB luciferase activity. For stability of PLGA particles encapsulating flavopiridol (E), NF-κB luciferase activity of microparticles loaded with flavopiridol after

storage at different temperatures for different time periods 0, 30, 60, and 90 days was examined. Data are presented as the mean ± S.E. ($n \geq 3$ independent experiments). The statistically significant differences were calculated in comparison to the control where the following symbols represent the stated levels of significance: * - $p<0.05$, ** - $p<0.01$, and **** - $p<0.0001$ as determined by a one-way analysis of variance (ANOVA), followed by Tukey's multiple-comparison test.

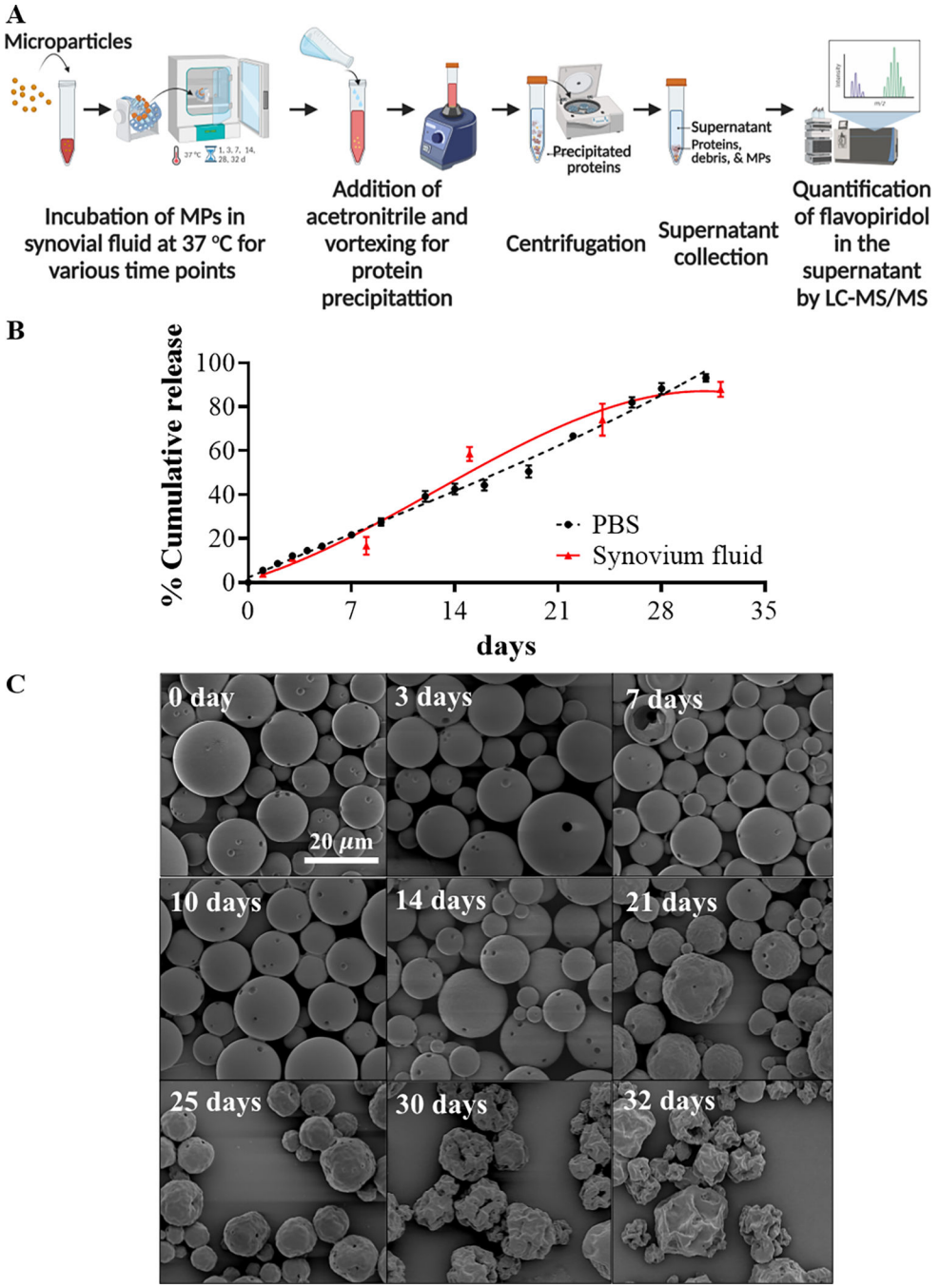

Figure 3. Release kinetic of FPs.

Schematic depicting study design for release kinetics of flavopiridol-loaded microparticles (A). Release profile of flavopiridol-loaded MPs in human synovial fluid in PBS and synovial fluid (B). SEM images of FPs at designated time points during *in vitro* release measurements. The scale bar (in white) represents 20 μm (C).

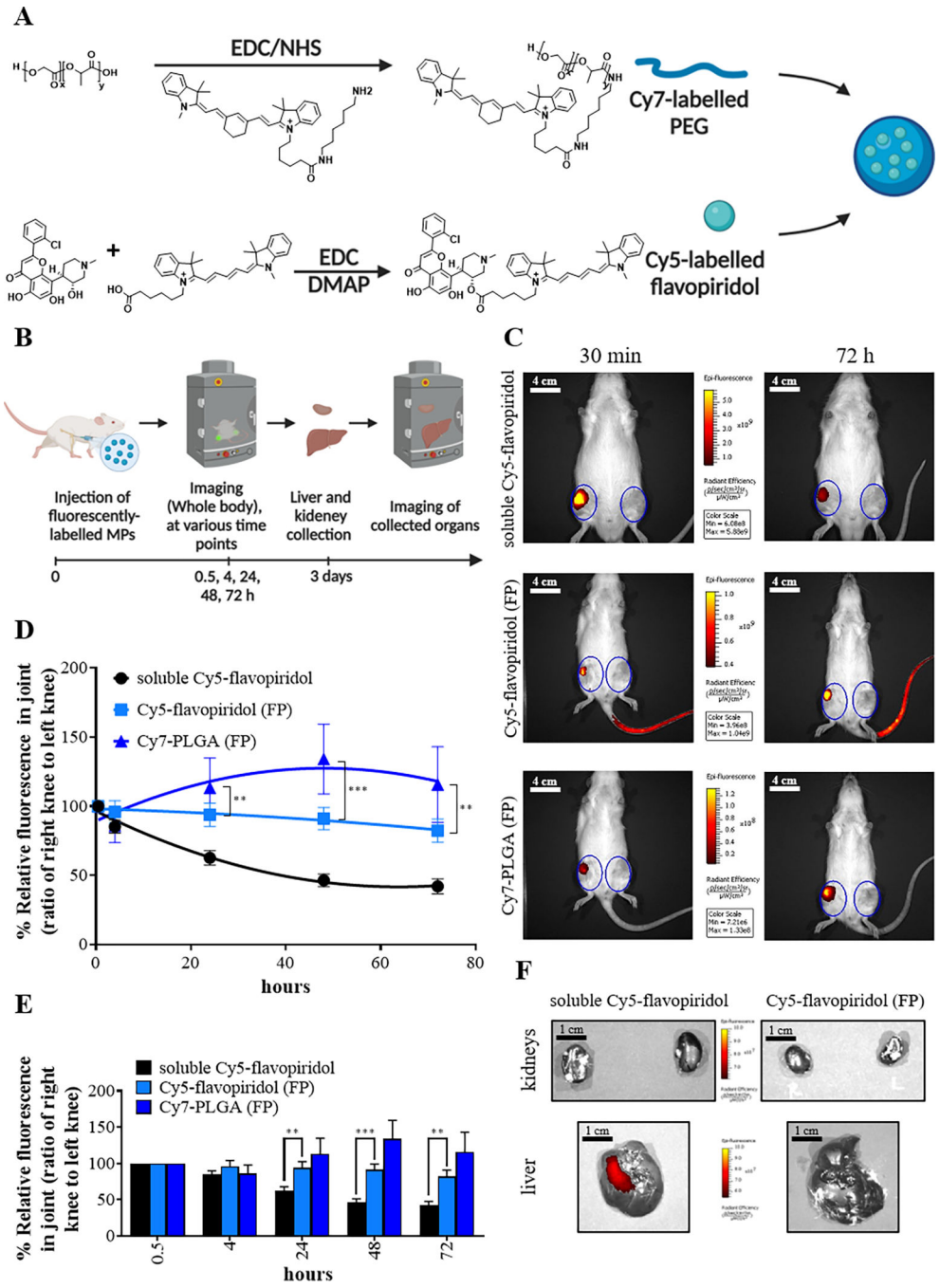

Figure 4. Biodistribution of Flavopiridol-loaded microparticles following intra-articular injection in rats.

Steps for chemical conjugation of Cy7-labelled PLGA and Cy5-labelled flavopiridol (A). A schematic depictive the approach for the FP biodistribution study (B). Representative IVIS image of rats after injection with microparticles or soluble flavopiridol are shown. The image is a merged picture of fluorescent signal in color and a grayscale picture of the rats. (C). The scale bar (in white) represents 4 cm (C). The fluorescence intensities were used to calculate the ratio of right knee to the left knee which were plotted to represent clearance of fluorescently-labeled FPs and Cy5-labelled flavopiridol from rat knees (D-E).

Representative IVIS image of livers and kidneys harvested from rats at 72 hours after intra-articular injection of either flavopiridol-loaded microparticles or soluble flavopiridol are shown (F). The scale bar (in black) represents 1 cm (F). Data are presented as the mean ± S.E. ($n \geq 4$ for experimental group) and the following symbols represent the stated levels of significance: ** - $p<0.01$, *** - $p<0.001$ as determined by unpaired t-test or Mann-Whitney U test depending on the type of data distribution.

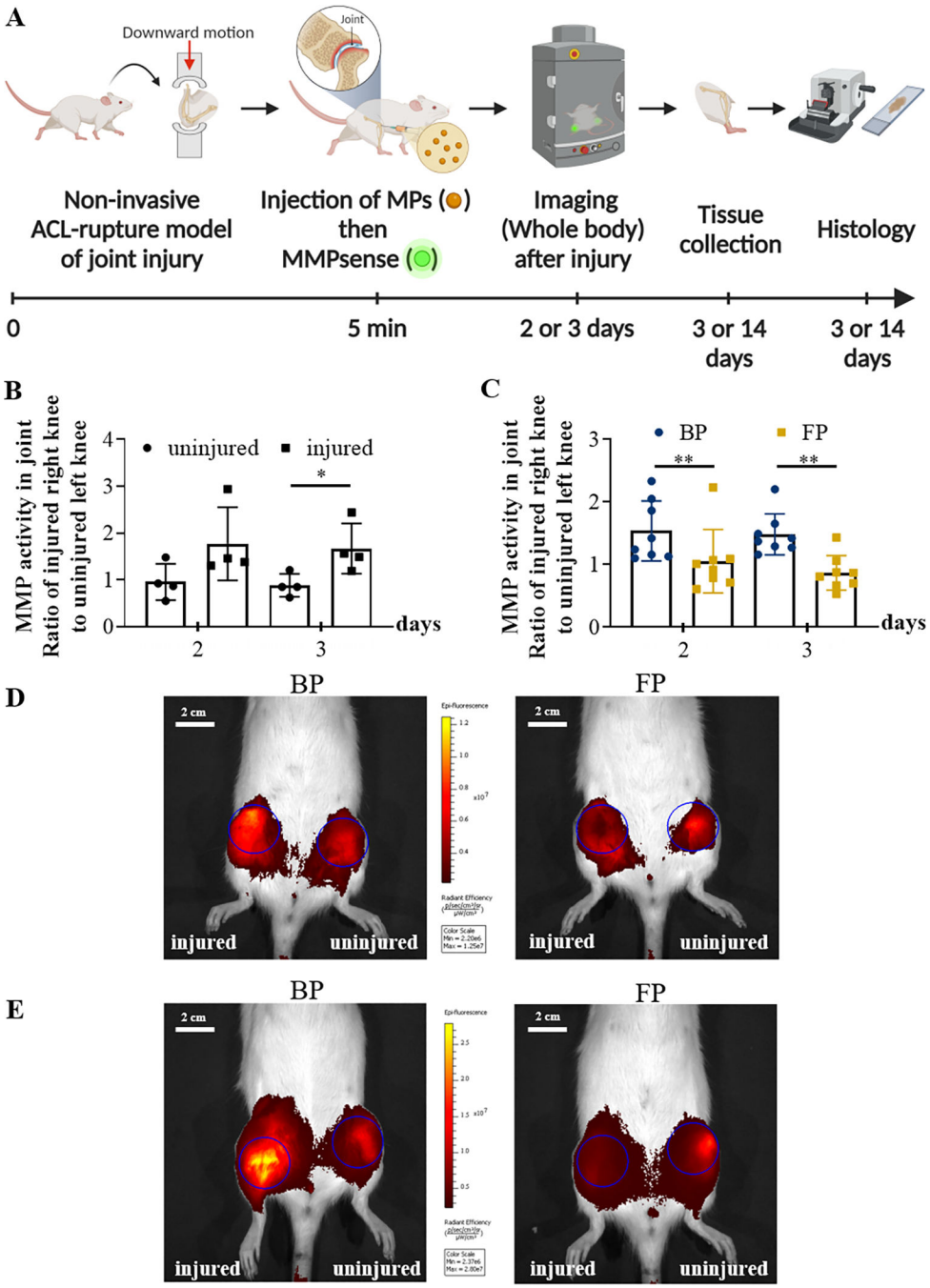

Figure 5. Flavopiridol-loaded microparticles reduces MMP activity in PTOA joints.

A schematic depicting the experimental approach for generation of non-invasive PTOA and *in vivo* imaging of MMP activity (A). The graph shows that MMP activity in injured knees (n=8) was significantly higher than the controls (uninjured; n=4) (B). A third cohort of rats (n=8) were subjected to noninvasive ACL rupture in their right knees and subsequently injected with either BPs or FPs (0.8 mg particles in 50 uL PBS). MMPsense were administered on both knees and the whole rats were imaged by IVIS on days 2 and 3 after injury (C). Representative IVIS images of knees after MMPSense750 injection are

shown (D, E). The images are merged pictures of the fluorescent signal in color and a grayscale picture of the mouse. Blue circles on both knees are ROI with the same shape and size for each specimen. The scale bar (in white) represents 2 cm (D, E). Data in graphs (B, C) are presented as the mean ± S.E. ($n \geq 4$ independent experiments), and the following symbols represent the stated levels of significance: * - $p<0.05$, ** - $p<0.01$, as determined by unpaired t-test or Mann-Whitney U test depending on the type of data distribution.

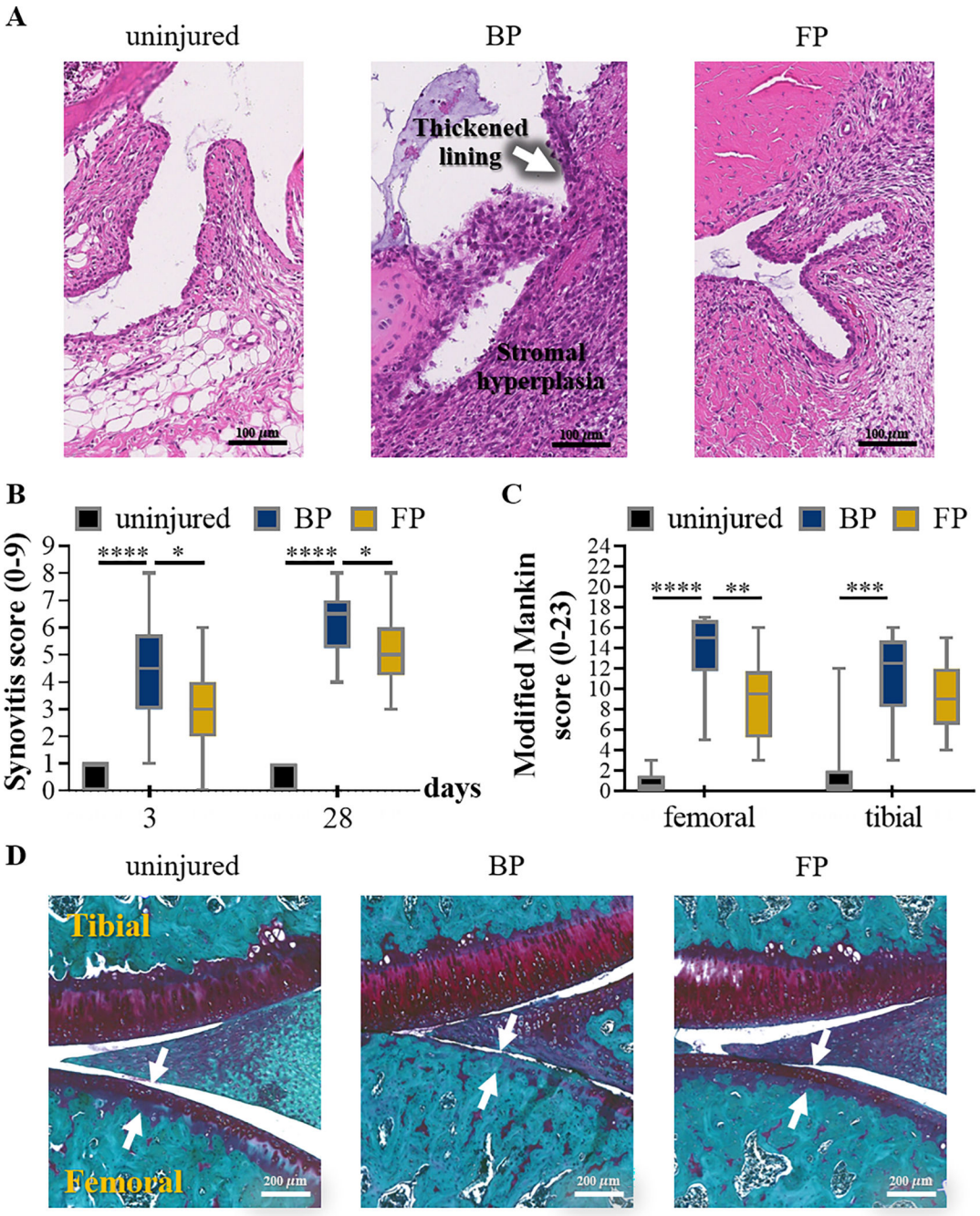

Figure 6. Efficacy of flavopiridol-loaded microparticle therapy in a rat PTOA model.

Representative images of synovial tissues stained with hematoxylin/eosin at day 3 after ACL injury. FP treatment reduced the level of synovitis, compared to vehicle-treated animals (A). The scale bar (in black) represents 100 μm (A). Synovitis in all animal groups were assessed by 2 blinded observers as described in the experimental procedures. The individual synovitis scores were used in the box plots (B). FP treatment significantly reduced the levels of synovitis, both at the 3- and 28-day time points (B). Data are used in the box plots (n = 8/ group with 4 contralateral uninjured knees from each group serving as controls),

and the following symbols represent the stated levels of significance: * - $p<0.05$, **** - $p<0.0001$, as determined by unpaired t-test or Mann-Whitney U test depending on the type of data distribution. Safranin O stained cartilage and bone in dark purple and blue color, respectively. In vehicle-treated animals, injury caused a loss of cartilage, more prominently at the femoral than the tibial condyle. Whereas, FP treatment slightly reduced cartilage loss. The severity of osteoarthritis was semi-quantitatively assessed by the Modified Mankin score by 2 blinded observers as described in the experimental procedures (C). The individual osteoarthritis scores with S.E. determined at 4-week post-injury are shown. Drug treatment reduced the Modified Mankin scores, indicating a reduction in osteoarthritis severity. Data are used in the box plots (n=5/control group, and n=6/vehicle- and drug-treated groups), and the following symbols represent the stated levels of significance: ** - $p<0.01$, *** - $p<0.001$, and **** - $p<0.0001$ as determined by unpaired t-test or Mann-Whitney U test depending on the type of data distribution. Representative images of joint tissues stained with Safranin O at 4 weeks after ACL injury are shown with the scale bar (in white) representing 200 μm (D).

Table 1.

Properties of flavopiridol encapsulated PLGA particles

particles	formulation	method	size, μm	size, SD	% loading efficiency	mmol flavopiridol/mg particle	% yield
Blank[b]	SE	vortex	11.7	8	-	-	50
Blank[b]	SE	nanoassemblr	15	14	-	-	23
flavopiridol[a]	SE	proprietary	14.9	7.7	50	2.96E-05	
flavopiridol[b]	SE	vortex	17	14	36	2.11E-05	
flavo-Cy5-1X[b]	SE	vortex	14.4	11.3	99	1.48E-05	
flavo-Cy5-2X[b]	SE	vortex	14.1	10.5	99	2.87E-05	
flavo-Cy5-1X[b]	SE	nanoassemblr	11.8	11.1	96	9.17E-06	
flavo-Cy5-2X[b]	SE	nanoassemblr	12.3	12	63	1.30E-05	

SE = single emulsion

1X = 1.2 % (g/g) of Cy5-labelled flavopiridol used

2X = 2.4 % (g/g) of Cy5-labelled flavopiridol used

[a]provided by Tesio Pharmaceuticals

[b]provided by Lewis laboratory